Comparison of DTI Fiber Tracks with Light Microscopy of Myelinated Fibers

A. S. Choe[1,2], X. Hong[1,2], D. C. Colvin[1,2], I. Stepniewska[3], Z. Ding[1,2], and A. W. Anderson[1,2]

[1]Vanderbilt University Institute of Imaging Science, Vanderbilt University, Nashville, TN, United States, [2]Department of Biomedical Engineering, Vanderbilt University, Nashville, TN, United States, [3]Department of Psychology, Vanderbilt University, Nashville, TN, United States

Introduction

Since the initial findings made by Hahn [1] and then Carr and Purcell [2] that one could use NMR methods to measure the effects of molecular diffusion, applications of the technique have become increasingly widespread. Nowadays diffusion imaging has established itself as an effective tool that can be used to analyze tissue microstructure noninvasively [3]. One of the most powerful applications of diffusion imaging is fiber tracking, which enables one to study white matter architecture. Several different fiber tracking methods exists, such as FACT (fiber assignment by continuous tracking) [4, 5] and probabilistic fiber tracking [6]. Several challenges exist for fiber tracking, including ambiguous fiber direction due to low anisotropy and noise, the tendency to accumulate error over the length of the fiber, and the problem of distinguishing crossing and kissing fibers. In this abstract we observe several causes of fiber tracking errors.

Methods

A fixed non-human primate (owl monkey) brain was scanned, ex vivo, then sectioned coronally and stained for myelin. Three major datasets were acquired: DT-MRI, tissue blockface photographs, and high resolution light micrographs. Diffusion images were obtained on a 9.4T Varian scanner using a multi-slice, pulsed gradient spin echo sequence (22 weighting directions, b = 0 and 1309 s/mm^2 , TE = 31 ms, TR = 17.1 s, 128 x 128 x 132 image volume matrix, 0.3 x 0.3 x 0.3 mm^3 voxels resolution). From the diffusion MRI dataset, tensors and fiber orientation distribution (FOD) functions were obtained. The FOD for each voxel was calculated using the FORECAST spherical deconvolution method [7]. Fiber tracking was performed using DtiStudio [8], where fibers were tracked from every voxel in the brain. The fibers were then transferred to the micrograph image space through a series of registration steps, as described previously [9, 10]. Diffusion data were registered with light micrographs using blockface photographs as an intermediate step and both rigid [11] and nonrigid transformations calculated by the Adaptive Bases Algorithm (ABA) [12]. An additional non-rigid registration step using the thin plate spline (TPS) algorithm [13] was performed for better accuracy.

Results

A tensor, FORECAST FOD, and rose plot of myelinated fibers in the corresponding patch of a micrograph in a region with coherent fiber structures (corpus callosum) are shown in Figure 1 (a), (b), and (c). Orientations of all three plots are consistent and the fiber tracks in Figure 1 (a) follow smoothly along the fiber paths shown in the micrograph. Figure 1(d) and (e) are images of a micrograph region with more complicated structure, obtained from a region near the intersection of the coronal radiata and corpus callosum. When DTI fiber tracks are overlaid, it can be seen in Figure 1(e) that DTI fiber tracks follow a direction intermediate between the two crossing paths (see the left edge of the images). A detailed look into a voxel within this region is taken in Figure 1(f), (g), and (h). Figure 1(h) is a rose plot of the FOD measured directly from the micrograph patch. It shows the two major peaks along the direction of the two true fiber paths. While the tensor and DTI fiber tracks in Figure 1(f) follow the diagonal fiber bundle, but not the horizontal one, the FORECAST FOD in Figure 1(g) shows the information from the two major pathways is not lost and may be recovered. It can also be seen in the left portion of Figure 1(e) that when major crossing of fibers occurs and the resolution is not high enough, fibers can step into a different bundle, as in this case where some fibers of the diagonal fiber bundle branch off to follow the horizontal fiber bundle.

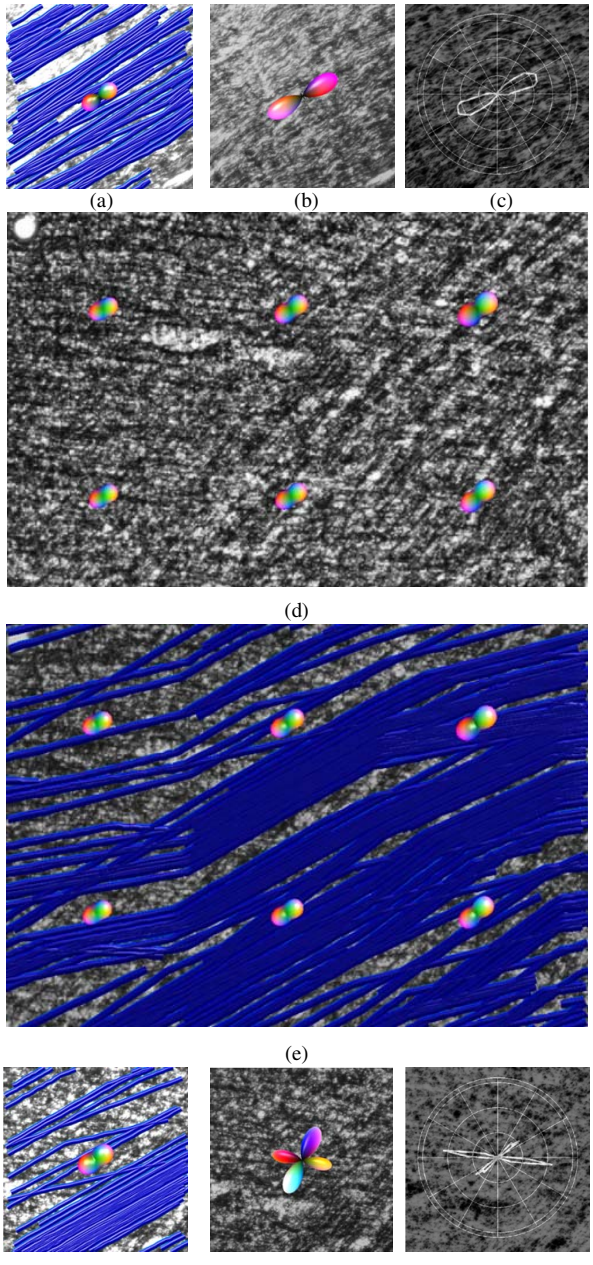

Figure 1. Fiber tracks and tensor (a), FORECAST FOD (b), and rose plot FOD (c) from a micrograph patch with coherent fiber structure, all overlaid on the micrograph patch. Tensors (d, e) and fiber tracks (e) from a region with less coherent fiber structure are overlaid on the micrograph, over a larger field of view. Detail of the fiber tracks and tensor (f), FORECAST FOD (g), and rose plot FOD (h) from the top-center region in (e).

Conclusion

The major challenges of DTI fiber tracking can be observed and quantified at the microscopic level. As the number of applications of DTI increases, it is especially important to understand the limitations and strengths of the technique. Our findings show that comparing the DTI fiber tracks with the gold standard fiber orientation and spread information provided by myelin stained sections reveals the relationship between DTI and actual microstructural properties of white matter. The ability of the FORECAST FOD to reveal complex fiber geometry suggests that this and similar techniques show promise as a basis for improved fiber tracking.

Acknowledgements

This work was supported in part by grants from the National Institute of Health (1RO1 EB002777, 1R01 NS058639, and 1S10 RR17799). The authors would like to thank Dr. Benoit Dawant for help with image registration, and Young Li for help with tensor reorientation.

References

[1] Hahn, E.L., Phys Rev, 1950(80): p. 580-594. [2] Carr, H.Y. and E.M. Purcell, 1954(80): p. 630–638. [3] Moseley, M.E., et al., Radiology, 1990. **176**(2): p. 439-45. [4] Mori, S., et al., Ann Neurol, 1999. **45**(2): p. 265-9. [5] Xue, R., et al., Magn Reson Med, 1999. **42**(6): p. 1123-7. [6] Zhang, F., et al., Med Image Comput Comput Assist Interv Int Conf Med Image Comput Comput Assist Interv, 2007. **10**(Pt 2): p. 144-52. [7] Anderson, A.W., Magn Reson Med, 2005. **54**(5): p. 1194-206. [8] Jiang, H., et al., Comput Methods Programs Biomed, 2006. **81**(2): p. 106-16. [9] Choe, A.S. *In 15th ISMRM*. 2007. Berlin, Germany. [10] Choe, A.S. In *16th ISMRM*. 2008. Toronto, Canada. [11] Maes, F., IEEE Trans Med Imaging, 1997. **16**(2): p. 187-98. [12] Rohde, G.K., IEEE Trans Med Imaging, 2003. **22**(11): p. 1470-9. [13] Wahba, G., 1990, Philadelphia: Society for Industrial and Applied Mathematics.